SECURITY CLASSIFICATION OF THIS PAGE *(When Data Entered)*

REPORT DOCUMENTATION PAGE		READ INSTRUCTIONS BEFORE COMPLETING FORM
1. REPORT NUMBER NRL Report 7676	2. GOVT ACCESSION NO.	3. RECIPIENT'S CATALOG NUMBER
4. TITLE *(and Subtitle)* APPLICATION OF THE *J* INTEGRAL TO CRACK INITIATION IN A 2024-T351 ALUMINUM ALLOY		5. TYPE OF REPORT & PERIOD COVERED This report completes one phase of a continuing NRL problem. 6. PERFORMING ORG. REPORT NUMBER
7. AUTHOR(s) C. A. Griffis and G. R. Yoder		8. CONTRACT OR GRANT NUMBER(s)
9. PERFORMING ORGANIZATION NAME AND ADDRESS Naval Research Laboratory Washington, D.C. 20375		10. PROGRAM ELEMENT, PROJECT, TASK AREA & WORK UNIT NUMBERS NRL Problem M01-24 RR 022-01-46-5431
11. CONTROLLING OFFICE NAME AND ADDRESS Department of the Navy Office of Naval Research Arlington, Va. 22217		12. REPORT DATE April 3, 1974 13. NUMBER OF PAGES 27
14. MONITORING AGENCY NAME & ADDRESS*(if different from Controlling Office)*		15. SECURITY CLASS. *(of this report)* Unclassified 15a. DECLASSIFICATION/DOWNGRADING SCHEDULE

16. DISTRIBUTION STATEMENT *(of this Report)*

Approved for public release; distribution unlimited.

17. DISTRIBUTION STATEMENT *(of the abstract entered in Block 20, if different from Report)*

18. SUPPLEMENTARY NOTES

19. KEY WORDS *(Continue on reverse side if necessary and identify by block number)*

J integral
Fracture resistance
Aluminum alloys
Fracture mechanics

20. ABSTRACT *(Continue on reverse side if necessary and identify by block number)*

The *J* integral has been successfully applied as a fracture initiation criterion for 2024-T351 aluminum alloy. A heat-tinting technique was used for quantitative measurement of crack extension at selected points on the load-deflection curve. In three-point bend tests incorporating six specimen configurations the critical *J* values (J_{Ic}) at the onset of crack movement differ by at most 15 percent and yield a mean K_{Ic} value of 30.9 ± 1.2 ksi/in.$^{1/2}$. The relationship between instantaneous *J* value and crack extension is independent of initial crack length over the range of crack sizes investigated. *J*-integral values associated with maximum load (5 to 15 percent crack growth), unlike J_{Ic}, show a strong dependence on specimen thickness.

DD FORM 1 JAN 73 1473 EDITION OF 1 NOV 65 IS OBSOLETE
S/N 0102-014-6601 |

SECURITY CLASSIFICATION OF THIS PAGE *(When Data Entered)*

CONTENTS

APPLICATION OF THE J INTEGRAL TO CRACK INITIATION IN A 2024-T351 ALUMINUM ALLOY

INTRODUCTION

Linear elastic fracture mechanics (LEFM) has been successful in analyzing the brittle fracture of high-strength materials where the plastic zone size at the tip of the flaw is small in comparison to the overall dimensions of the specimen or structural component (e.g., plastic zone size/plate thickness < 0.02). However most structures are fabricated from higher toughness, low- and intermediate-strength alloys, which greatly minimizes the likelihood of an unstable fracture at low, nominally elastic stress levels. Unfortunately there is no generally accepted practice whereby the fracture toughness of these more ductile materials may be quantitatively assessed and interpreted in terms of useful relationships between flaw size and load level under conditions of large-scale plasticity.

The J integral, formulated by Rice [1], has recently been proposed as a generalized fracture-initiation criterion applying under conditions of either localized or widespread plastic flow prior to crack extension. While the J integral is a measure of the amplitude of the plastic strain singularity at the crack tip, it is attractive for fracture characterization in that it may be readily measured without resorting to direct, tedious crack-tip analyses. Using small, fully plastic laboratory specimens, Begley and Landes [2,3] have demonstrated for low- and intermediate-strength steels that the J-integral value at the onset of crack movement J_{Ic} is independent of specimen geometry and consistent with prior LEFM characterizations using much larger specimens. These results, though quite encouraging, are by no means conclusive proof of the general validity of the J-integral approach, and the present investigation is intended to further document the utility of the J integral as applied to a somewhat less ductile (elastic-plastic) aluminum alloy.

THEORETICAL BACKGROUND

The J integral as defined by Rice [1] for two-dimensional problems is given by the contour integral

$$J = \int_{\Gamma} \left(W\, dy - \mathbf{T} \cdot \frac{\partial \mathbf{u}}{\partial x}\, ds \right), \tag{1}$$

where, as shown in Fig. 1, $\mathbf{u}$ is the displacement vector acting along any path Γ surrounding the crack tip and $\mathbf{T} = \boldsymbol{\sigma} \cdot \mathbf{n}$ is the surface traction vector defined with respect to the outward normal $\mathbf{n}$ on Γ. Arc length is denoted by s, and the strain energy density W is defined for nonlinear (or linear) elastic materials by

$$W(\epsilon_{mn}) = \int^{\epsilon_{mn}} \sigma_{ij}\, d\epsilon_{ij},$$

where σ_{ij} and ϵ_{ij} are the components of stress and strain respectively.

Manuscript submitted October 17, 1973.

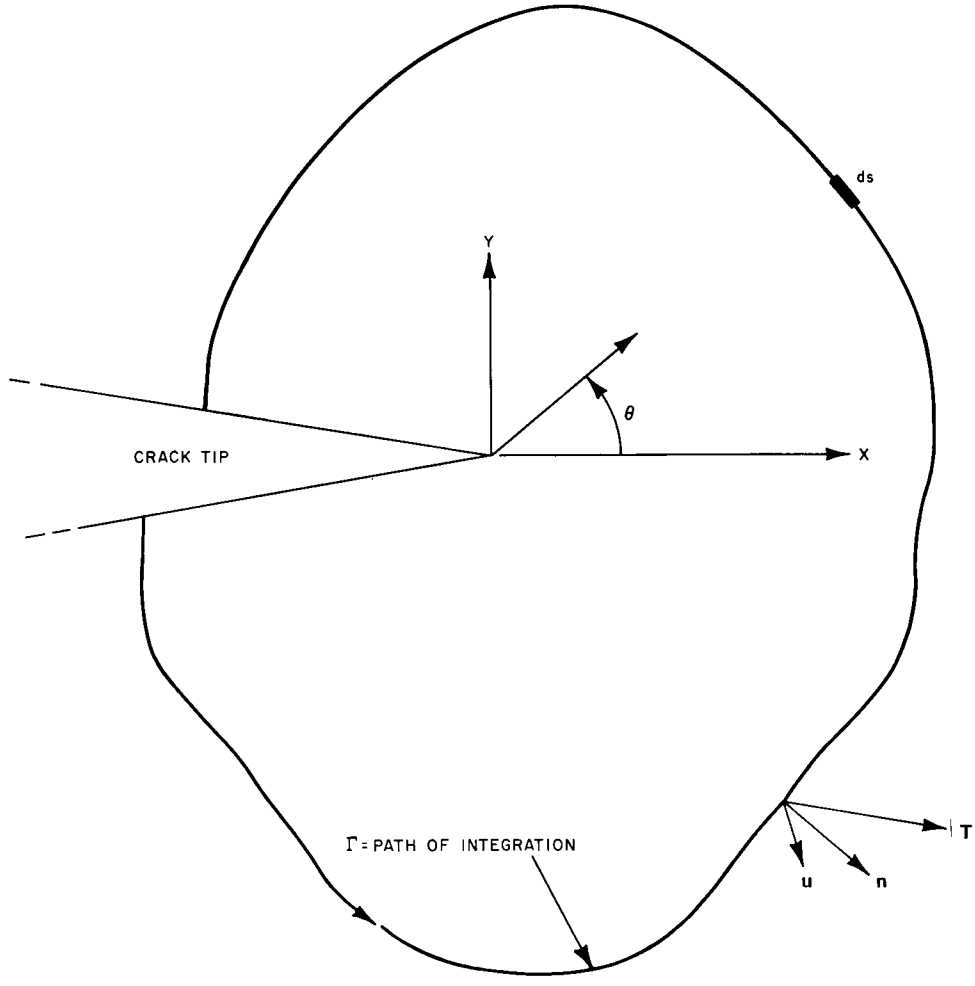

Fig. 1 — Crack-tip coordinate system, illustrating the parameters used in defining the J integral

Hutchinson [4] and Rice and Rosengren [5] have determined the nature of the stress and strain distributions at the tip of a crack for strain hardening materials which display a Ramberg-Osgood relationship between effective stress σ and effective plastic strain ϵ_p:

$$\sigma = \sigma_1 (\epsilon_p)^n ,$$

where the strain hardening exponent n varies from 0 to 1. McClintock [6] has combined these analyses with Rice's definition of the J integral, Eq. (1), and arrived at the following forms for the crack-tip stress and strain singularities:

$$\sigma_{ij} = \left[\frac{J}{\sigma_1 I(n)}\right]^{n/n+1} \frac{1}{r^{n/n+1}} \tilde{\sigma}_{ij}(\theta), \tag{2a}$$

$$\epsilon_{ij} = \left[\frac{J}{\sigma_1 I(n)}\right]^{1/n+1} \frac{1}{r^{1/n+1}} \tilde{\epsilon}_{ij}(\theta), \tag{2b}$$

where r and θ represent the in-plane polar coordinates (Fig. 1) and the functions $I(n)$, $\tilde{\sigma}_{ij}(\theta)$, and $\tilde{\epsilon}_{ij}(\theta)$ depend on the mode of crack opening and are given in Ref. 4 for plane stress and plane strain deformations. The important aspect of Eqs. (2) is that they provide a physical interpretation of the J integral as representing the amplitude of the stress and strain singularities under elastic-plastic conditions. Specification of the J-integral value and the appropriate flow properties, σ_1 and n, uniquely determines the crack-tip stress and strain fields. Thus adoption of the J integral as a fracture-initiation criterion is equivalent to stating that a crack will move when the local stress and strain environment at the crack tip attains a fixed severity. It must be pointed out however that Eqs. (2) are idealizations of the actual crack-tip behavior in that they are derived from a two-dimensional analysis based on infinitesimal displacements and assume a deformation theory of plasticity (nonlinear elasticity) in which strain hardening is governed by the Ramberg-Osgood relationship.

An important characteristic of the J integral is its path independence [1]. By using this fact and performing the integration about a contour Γ coincident with the boundary of the body, it can be shown [7] that the J integral can be interpreted in terms of the difference in potential energy dU between two identically loaded bodies having infinitesimally differing crack sizes da:

$$J = -\frac{1}{B}\frac{dU}{da}, \tag{3}$$

where B is the thickness and the potential energy is given by

$$U = \int_V W\, dV - \int_{S_T} \mathbf{T} \cdot \mathbf{u}\, dS. \tag{4}$$

In Eq. (4), V is the volume of the body and S_T represents that portion of the boundary surface over which the surface traction vector $\mathbf{T}$ is prescribed. If loading is to be measured in terms of displacements, then $S_T = 0$ and the second term of Eq. (4) vanishes. As shown

by Begley and Landes [2,3], Eqs. (3) and (4) can be used to experimentally define the dependence of J on deflection and crack size by a straightforward analysis of load-versus-deflection records.

For plane strain linear elastic behavior, J_{Ic} as defined by Eq. (3) becomes identical to the critical strain energy release rate G_{Ic}, which is in turn related to the elastic stress intensity factor K_{Ic} used in LEFM:

$$J_{Ic} = G_{Ic} = \frac{(1 - \nu^2)}{E} K_{Ic}^2, \tag{5}$$

where E and ν are Young's modulus and Poisson's ratio respectively. Equation (5) provides a check on the integrity of J_{Ic} numbers measured under elastic-plastic or fully plastic conditions. Such values, if meaningful, must be consistent with K_{Ic} numbers measured under linear elastic conditions as given by ASTM Standard E399-72 [8].

EXPERIMENTAL PROCEDURE

Material

To further evaluate the J integral as a fracture criterion a series of three-point bend tests were performed using a 2024-T351 aluminum alloy having the room-temperature mechanical properties (T-L orientation) given in Table 1a and chemistry limits given in Table 1b. This alloy was obtained from the Aluminum Company of America in the form of a 1-in.-thick plate and was tested at room temperature in the as-received condition (solution treated followed by cold work prior to natural aging). A light micrograph and electron fractograph of the material in the as-received condition are shown in Fig. 2. As expected, the fracture mode in air at room temperature is microvoid coalescence accompanied by substantial stretching.

Geometry and Preparation of Specimens

Figure 3 shows the dimensions of the various bend specimens employed. Specimens having thicknesses B of 0.93, 0.50, and 0.25 in. were fabricated by machining equal amounts of material from each surface of the as-received plate. For each thickness, J_{Ic} values were determined using specimens having initial crack lengths a_0 of approximately $0.47W$ and $0.60W$. The cracks were oriented parallel to the rolling direction and were generated by first slotting the specimens to a depth of $0.2W$ followed by fatigue cracking to the depths given in Fig. 3. The specimens were fatigue precracked in cantilever bending at a maximum ΔK level of 15 ksi$\sqrt{\text{in.}}$. For documenting the extent of crack movement under rising load, from six to 12 specimens were prepared for each of the six specimen configurations. The 0.25-in.-thick and 0.50-in.-thick bend bars are nearly geometrically similar in planar as well as thickness dimensions, whereas the 0.93-in.-thick and 0.50-in.-thick specimens have nearly the same in-plane dimensions.

Table 1a
Mechanical Properties of 2024-T351 Aluminum

Property	Value
Yield strength, σ_y	48.4 ksi
Tensile strength	70.5 ksi
% RA	23.5
% elongation (1.40 in.)	21.6
Young's modulus, E	11.5×10^3 ksi
1-in. DTE, 30°F	350 ft-lb

Table 1b
Chemical Composition
of 2024-T351 Aluminum

Element	Content* (wt-%)
Fe	0.50
Cu	3.8 — 4.9
Mn	0.30 — 0.9
Mg	1.2 — 1.8
Cr	0.10
Zn	0.25
Others	0.15
Al	Balance

*Maximum except when shown as a range.

Specimens with machined notches (root radius = 0.02 W) were used to experimentally determine the dependence of the J integral on midspan deflection δ and crack size a. Rounded notches were used to forestall stable crack growth during loading. For each thickness six calibration specimens were employed having a/W ratios ranging from 0.25 to 0.70. The experimentally determined J-integral calibration was compared with an analytical estimate given by Bucci et al. [9].

Test Apparatus and Instrumentation

All bend tests were conducted at room temperature using the apparatus shown schematically in Fig. 4. Crack mouth opening (CMO) and midspan deflection δ were simultaneously recorded as a function of applied load P using two X-Y recorders. Both

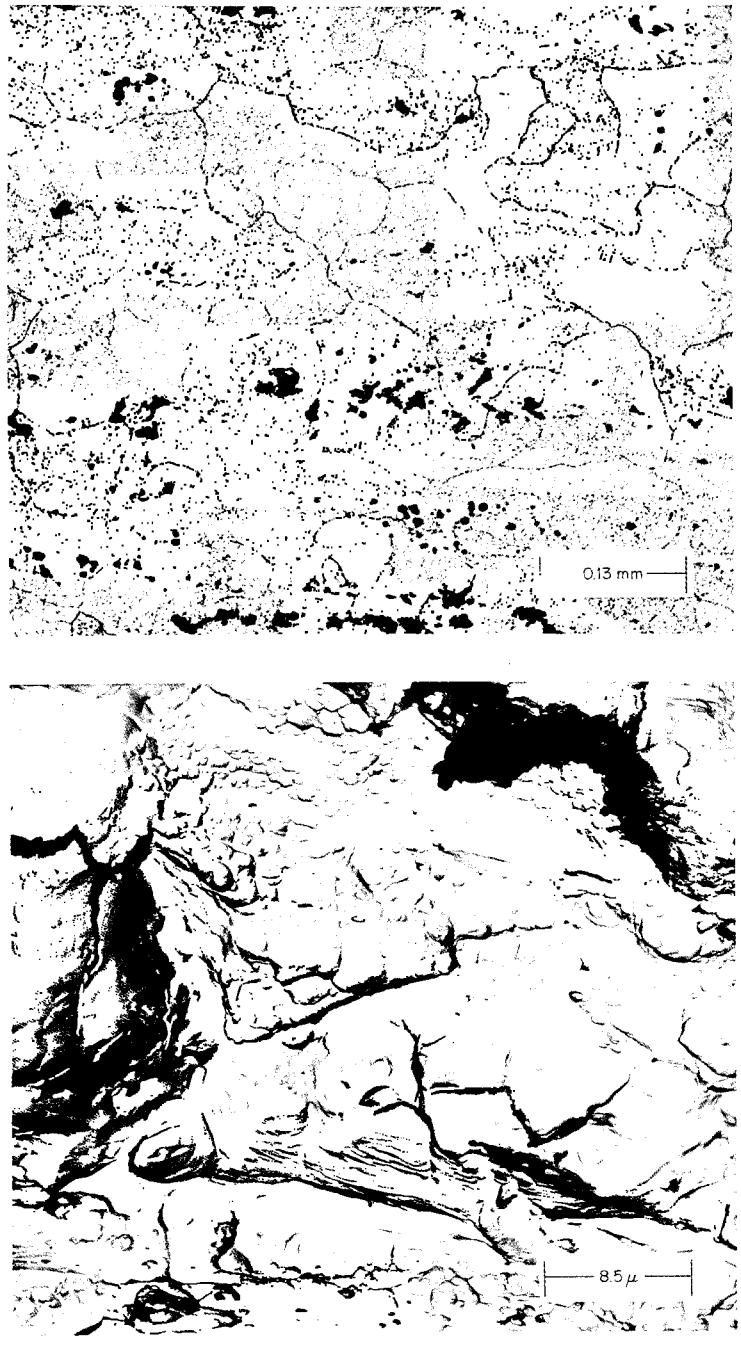

Fig. 2 — Light micrograph and electron fractograph of 2024-T351 aluminum in the as-received condition at room temperature

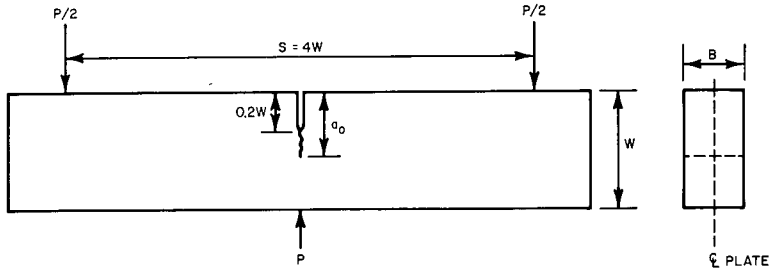

FATIGUE-CRACKED SPECIMENS

B(IN.)	W(IN.)	a_o/W
0.925	1.500	0.584 ± 0.006
0.925	1.500	0.449 ± 0.007
0.500	1.500	0.597 ± 0.007
0.500	1.500	0.466 ± 0.006
0.250	0.750	0.594 ± 0.006
0.250	0.750	0.468 ± 0.007

NOTCHED CALIBRATION SPECIMENS
(ROOT RADIUS = 0.02 W)

B(IN.)	W(IN.)	a_o/W
0.925	1.500	0.25 → 0.70
0.500	1.500	0.25 → 0.70
0.250	0.750	0.25 → 0.70

Fig. 3 — Dimensions of the three-point bend specimens

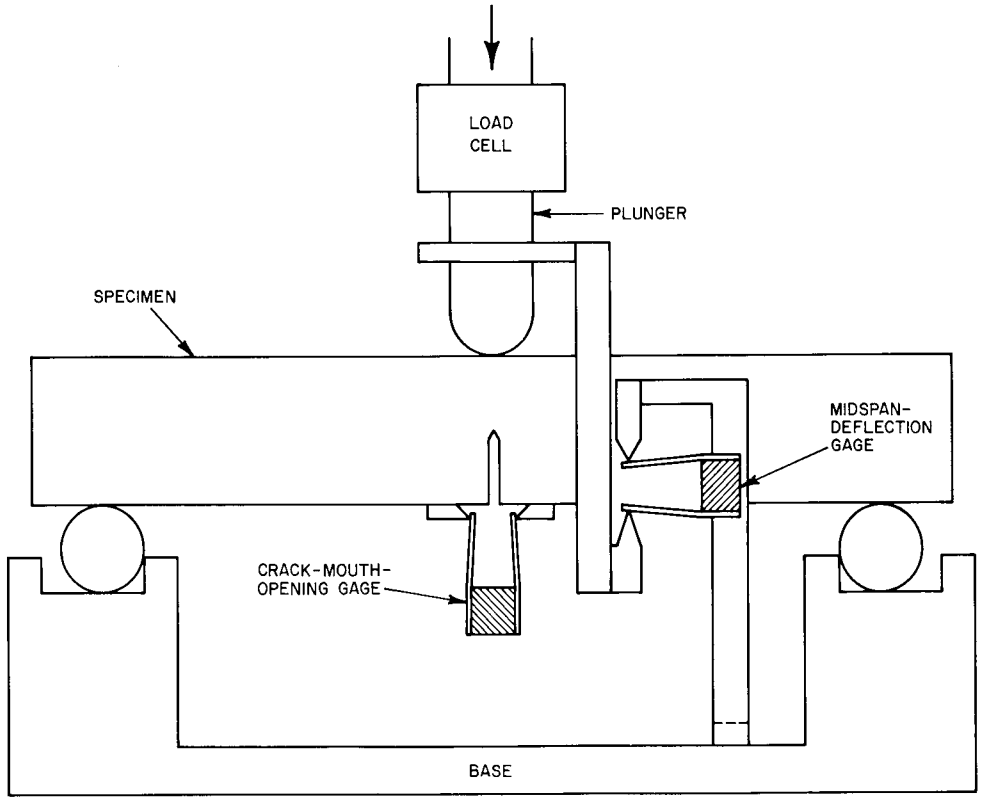

Fig. 4 — Schematic diagram of bend apparatus indicating midspan deflection and crack mouth opening gages

displacements were measured using double-cantilever beams fitted with a four-arm strain-gage bridge circuit as detailed in Ref. 10. For CMO measurement a beam gage was clipped to knife edges attached to the tension surface of the specimen, and for δ measurement a gage was placed between knife edges secured to the load plunger and support base respectively. The distance between rollers in the bend tests was maintained at 4 times the specimen height W.

Elastic deflections of the bend jig (rollers, plunger, and base) were determined by loading an unnotched rectangular bar within the elastic range and subtracting the midspan deflection as given by simple beam theory [11] from the measured deflection. The total bend-jig deflection amounted to approximately 4.1×10^{-4} in./kip* and was used to convert the measured deflections to actual specimen deflections for both notched and precracked specimens. This correction was employed to enable a comparison between the experimental and analytical calibrations, in that the latter deal exclusively with specimen deflections.

Crack Growth Measurement

Inasmuch as the J integral is currently being considered primarily as a fracture-initiation criterion, the extent of crack growth as a function of applied load must be monitored in elastic-plastic materials where appreciable stable growth may precede maximum load. To define the amount of cracking at selected points (up to and slightly beyond maximum load) on the load-versus-deflection records, identical specimens were loaded to successively larger deflections, unloaded, heat tinted, and subsequently broken apart. It was determined that adequate heat tinting could be obtained by heating the specimen in a circulating air furnace at 950°F for 18 to 36 hours, followed by air cooling. The longer heating times were required for specimens which had received the least amount of bending, presumably because the accessibility of air to the tip of the fatigue crack was more restricted. Following heat tinting, the degree of crack extension was determined by averaging the amounts of crack growth observed at the quarter-thickness positions. Crack-extension measurements were made to within ±0.002 in. using a stereomicroscope at 7 to 30 diameters magnification.

RESULTS AND DISCUSSION

J-Integral Calibration

The J-integral calibration was derived from experimentally determined load-versus-deflection records of bluntly notched bars using the method developed by Begley and Landes [2,3]. The procedure is illustrated in Figs. 5, 6, and 7 for the case of the 0.50-in.-thick specimens and is based on the definition of the J integral as expressed by Eq. (3): $JB = -dU/da$. First, a family of six diagrams of load P versus deflection δ (corrected for bend jig deflection) are measured for a series of specimens having slightly different crack lengths a_0 (Fig. 5). Since the deformation in the specimens is to be measured in terms of

*This value applies to the bend jig used in testing the 0.50-in.-thick and 0.93-in.-thick specimens. No significant deflections were observed in the jig used for the 0.25-in.-thick bars.

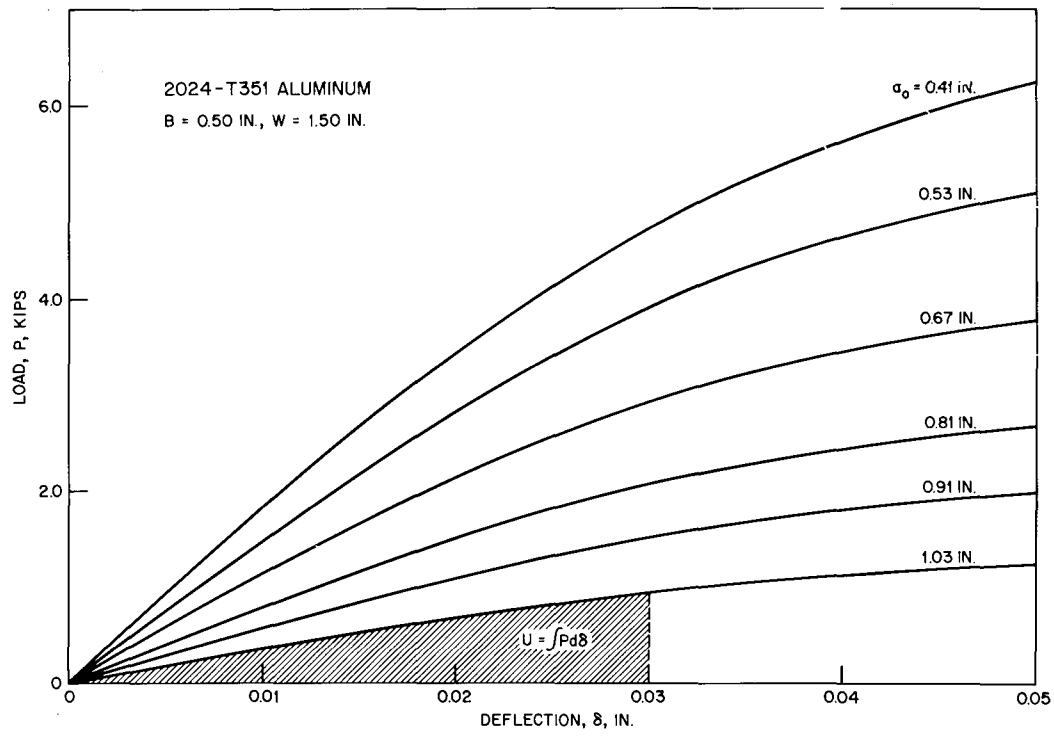

Fig. 5 — Load-versus-deflection diagrams for bluntly notched 2024-T351 aluminum calibration specimens (B = 0.50 in., W = 1.50 in.)

deflection, the potential energy U is simply the area under the load-versus-deflection record. By use of Simpson's rule the area under each curve is determined at several values of deflection, such as δ = 0.01, 0.02, . . ., 0.05 in. These values of U are then plotted versus crack size a_0 for the various δ values selected (Fig. 6). Finally the slopes of these curves, $dU/da = -JB$, are graphically measured as a function of δ for selected values of a_0. The solid curves of Fig. 7 show the resulting dependence of J/W on δ/W and a_0/W (J, δ, and a_0 are normalized with respect to specimen height W). Although the calibration shown in Fig. 7 was determined using 0.50-in.-thick specimens, nearly identical results were obtained for the 0.25-in.-thick and 0.93-in.-thick specimens. This is expected in the case of the 0.25-in. specimens on the basis of geometric similitude considerations and suggests that the flow behavior in the 0.50-in.-thick and 0.93-in.-thick bend bars is essentially two dimensional (thickness independent).

The dashed curves of Fig. 7 represent the estimated J-integral calibration according to the analytical method described in Ref. 9. Briefly, this technique involves modification of the elastic compliance formulas given by LEFM by augmenting the actual crack length by an amount equal to the plastic zone size.* This enables the (nonlinear) load-versus-deflection diagram to be approximated analytically, whereupon the J-integral calibration is determined by following exactly the same procedure as used for the experimental P-versus-δ curves. The comparison between experimental and analytical (plane stress) calibrations shown in Fig. 7 is reasonably good; throughout the range of a_0/W and δ/W

*Either a plane-stress or plane-strain approximation to the plastic zone size r_y may be employed. A plane-stress correction, namely, $r_y = (1/2\pi)(K/\sigma_y)^2$ was used in Fig. 7.

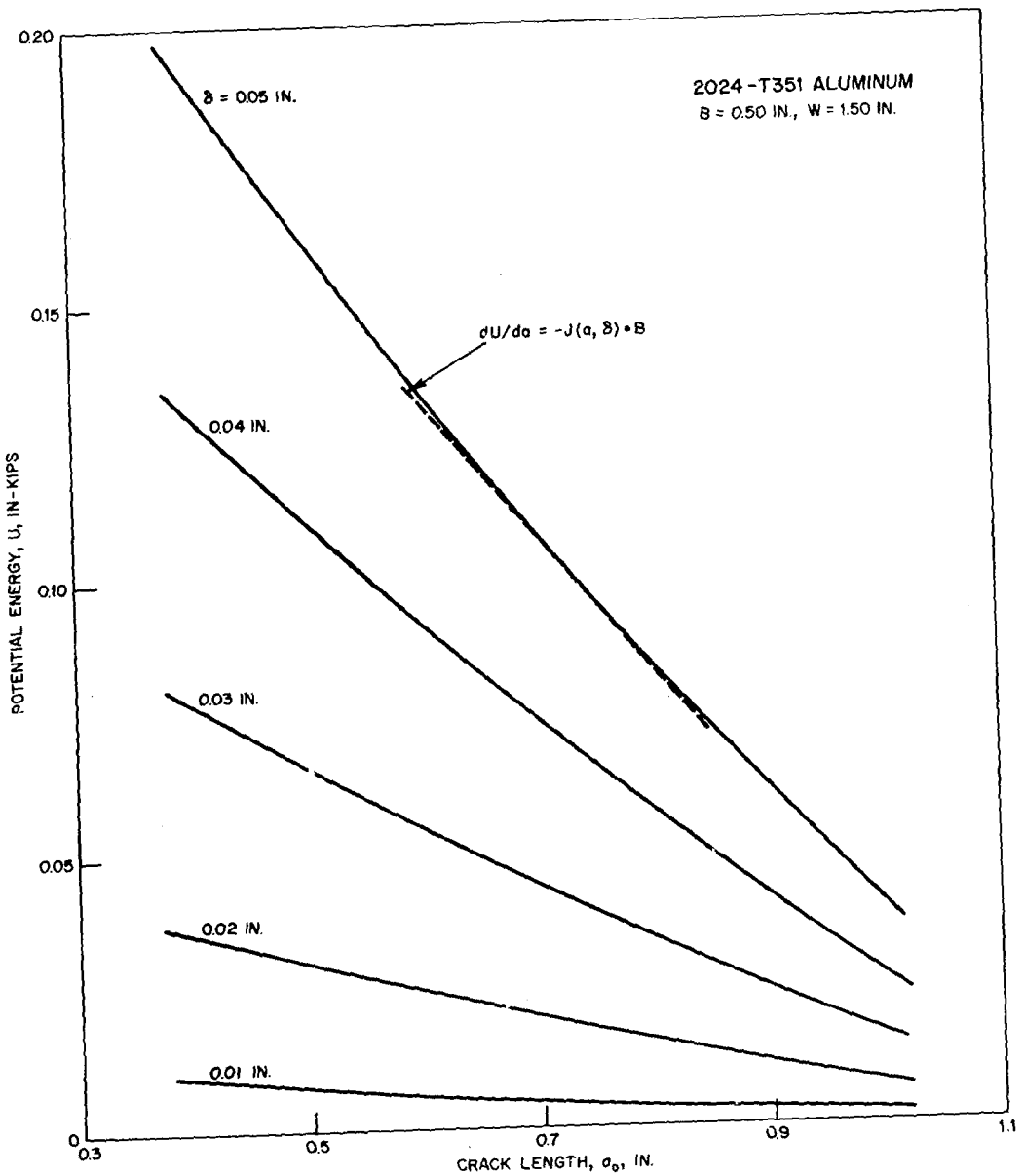

Fig. 6 — Potential energy versus crack length for 2024-T351 aluminum at several values of midspan deflection δ as obtained from Fig. 5

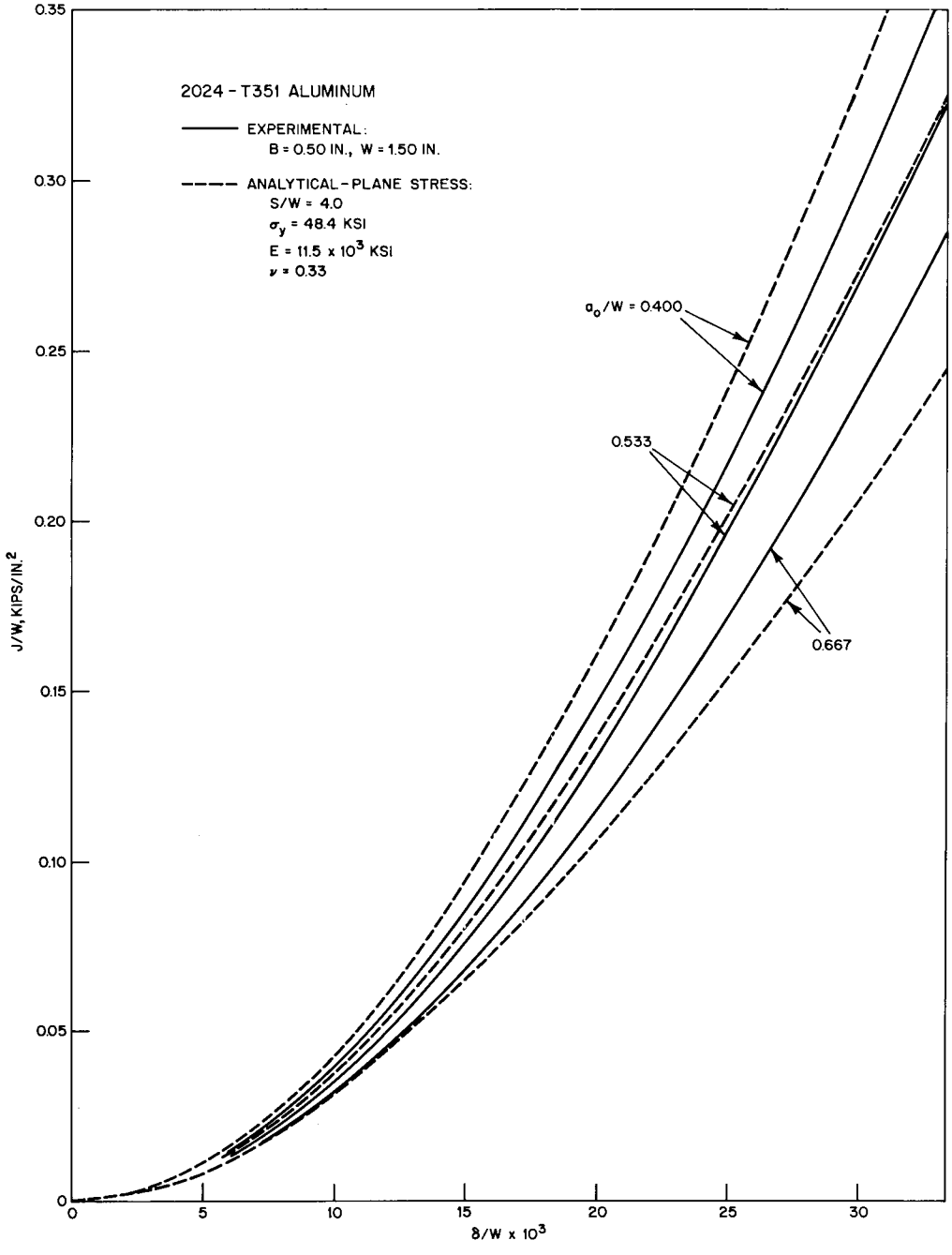

Fig. 7 — Experimental (from Fig. 6) and analytical J-integral-calibration curves for 2024-T351 aluminum bend specimens

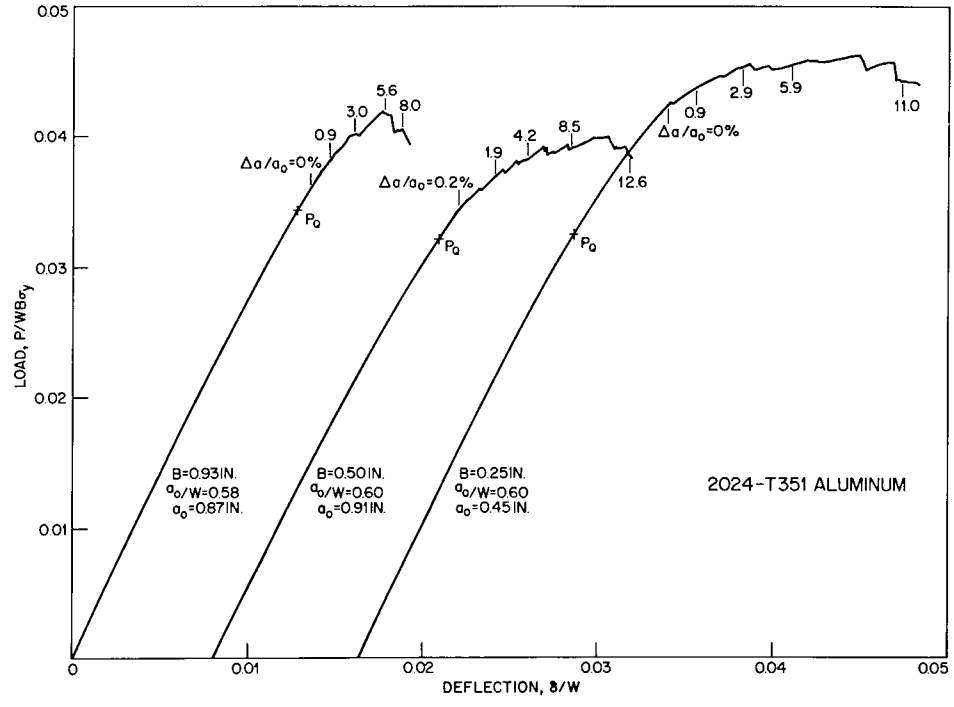

(a) $a_0/W \approx 0.60$

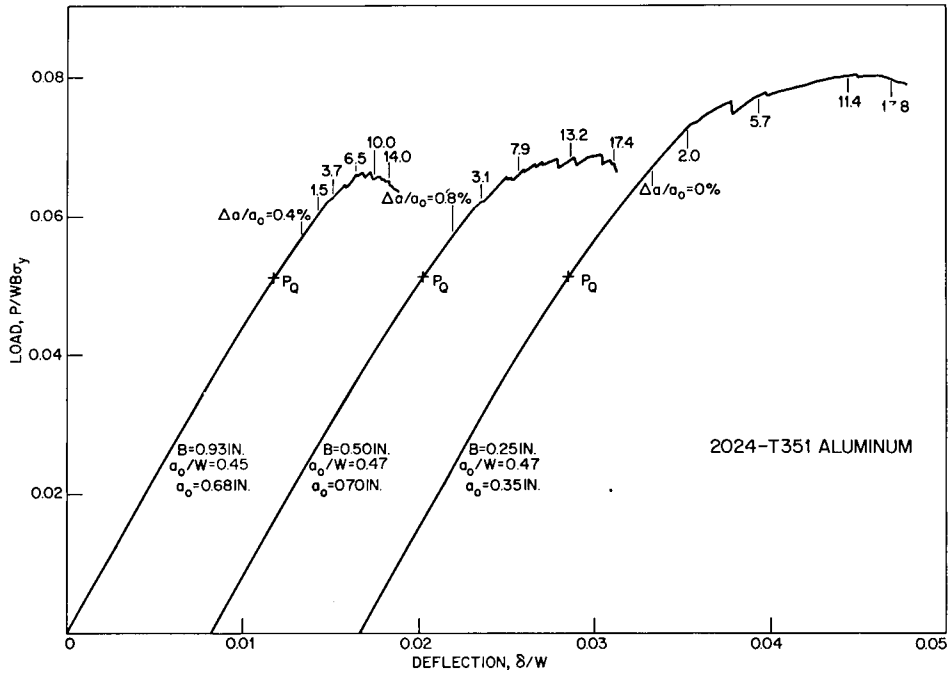

(b) $a_0/W \approx 0.47$

Fig. 8 — Load-versus-deflection diagrams for precracked 2024-T351 aluminum bend bars having thicknesses of 0.93, 0.50, and 0.25 in.

investigated the two methods agree to within about 10%. For a_0/W less than about 0.55 the analysis overestimates the experimental results, whereas the analysis yields conservative J values at higher a_0/W.

J Integral and K_Q Fracture Analysis

Figure 8a shows the experimental load-versus-deflection diagrams for the precracked specimens having thicknesses of 0.93, 0.50, and 0.25 in. with $a_0/W \approx 0.60$. Figure 8b is a similar plot pertaining to specimens of the same three thicknesses having $a_0/W \approx 0.47$. The percentage of crack extension, $100\ \Delta a/a_0$, as determined by heat tinting, is indicated for each specimen geometry at several locations on the load-deflection diagrams. Also shown on each curve is the load P_Q, defined by ASTM [8] as the load corresponding to a 5-percent secant offset on the curve of load versus crack mouth opening. This load is used to obtain a K_Q value, which in turn may be regarded as a valid K_{Ic} number, provided the amount of plasticity at P_Q is small and the rate of crack extension above P_Q is rapid:

$$B,\ a_0,\ W - a_0 > 2.5(K_Q/\sigma_y)^2$$

and

$$P_{max}/P_Q < 1.10.$$

As shown in Table 2 these criteria are not met for any of the specimen configurations tested, and as expected the indicated K_Q values display substantial variation with specimen size. It is also apparent in Fig. 8 and Table 2 that the load P_Q falls well below that at which crack extension begins for at least three of the six specimen configurations. These considerations demonstrate conclusively that K_Q cannot be meaningfully employed for fracture characterization in this alloy tested under the present conditions.

The load-versus-deflection diagrams in Fig. 8 indicate that crack extension commences below P_{max} and that initial crack movement is not generally accompanied by a detectable pop-in on the loading curve. The crack growth process, as revealed by heat tinting, is shown in Fig. 9 for specimens having thicknesses of 0.93, 0.50, and 0.25 in. with $a_0/W \approx 0.47$. (Load-deflection diagrams for these specimens are given in Fig. 8.) Crack extension first appears in the central portion of the specimen, generally between the $B/4$ and $3B/4$ positions, where the constraint is maximized. Upon further loading the crack front usually assumes a parabolic shape, with the maximum extension occurring close to the specimen midthickness. In several instances however a lobated front was observed, with the maximum penetration of the crack front appearing at the $B/4$ and $3B/4$ locations. This behavior was most prevalent in the 0.93-in.-thick specimens and is likely to reflect the existence of residual stresses imparted to the plate during cold reduction. No growth was apparent at the surface of any of the specimens prior to maximum load.

Figure 10 illustrates the details of the cracking process at a somewhat higher magnification. Crack initiation and subsequent growth are a heterogeneous process in which the crack front consists of numerous narrow protrusions into the uncracked ligament.

Table 2
K_Q Analysis for 2024-T351 Aluminum

B (in.)	a_0 (in.)	$W - a_0$ (in.)	K_Q (ksi$\cdot\sqrt{\text{in.}}$)	$2.5\left(\frac{K_Q}{\sigma_y}\right)^2$ (in.)	$\frac{P_{max}}{P_Q}$	$(\Delta a/a_0)_{P_Q}$ (%)
0.250	0.450	0.300	20.9	0.465	1.40	0
0.249	0.349	0.402	20.0	0.429	1.59	0
0.500	0.905	0.598	28.9	0.893	1.22	<0.2
0.501	0.706	0.797	28.5	0.869	1.34	<0.8
0.927	0.873	0.624	28.4	0.864	1.22	0
0.926	0.675	0.827	29.8	0.950	1.21	<0.4

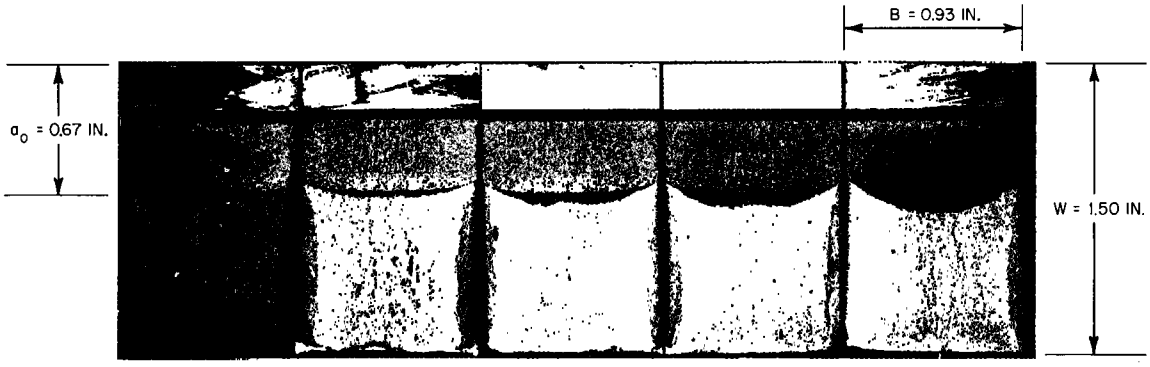

J (KSI-IN.)	0.0962	0.106	0.126	0.139	0.150
$\Delta a/a_0$ (%)	1.5	3.7	6.5	10.0	14.0

(a) 0.93-in.-thick specimens

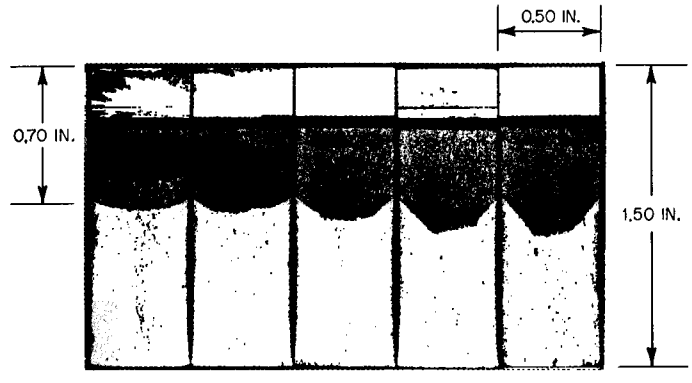

J (KSI-IN.)	0.0951	0.118	0.149	0.194	0.239
$\Delta a/a_0$ (%)	0.8	3.1	7.9	13.2	17.4

(b) 0.50-in.-thick specimens

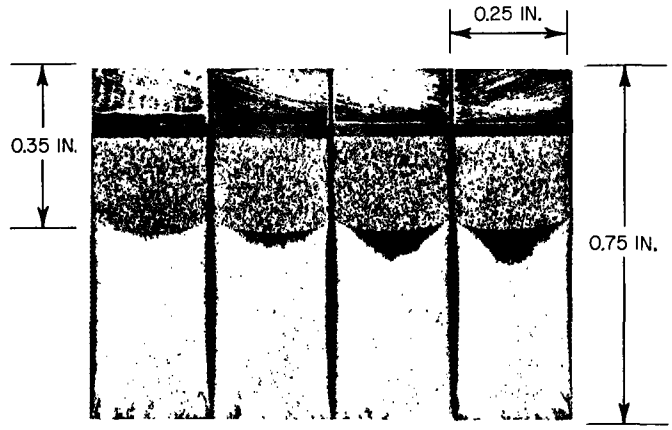

J(KSI - IN.)	0.103	0.127	0.180	0.208
$\Delta a/a_0$ (%)	2.0	5.7	11.4	13.8

(c) 0.25-in.-thick specimens

Fig. 9 — Crack extension as revealed by heat tinting for 2024-T351 aluminum specimens having $a_0/W \approx 0.47$

Figure 9 also shows the J-integral values associated with the indicated amounts of average crack extension. The cited J numbers were computed using the experimental J-integral calibration (Fig. 7) according to the instantaneous crack sizes $a_0 + \Delta a$ and the measured deflections (corrected for bend jig displacement). Plots of J versus Δa are shown for the three thicknesses investigated in Fig. 11. Each plot contains data for specimens having a_0/W ratios of approximately 0.47 and 0.60. To a good first approximation the J-versus-Δa relationships are independent of initial crack size a_0, and the smooth curves shown are intended to represent the best fit to the data for each thickness. To evaluate the J integral as an initiation criterion, two definitions of crack initiation were considered: 1-percent crack extension ($\Delta a = 0.01\ a_0$) and incipient crack movement defined by extrapolation of the J-versus-Δa curves to $\Delta a = 0$.

These definitions, though somewhat arbitrary, are consistent with the 2-percent (maximum) "effective" crack extension criterion currently used by ASTM [8] for linear elastic fracture. The location on the J-versus-Δa curves representing initiation according to each criterion are indicated in Fig. 11, and the associated critical J-integral values (J_{Ic}) are listed in Table 3. Also shown in Table 3 are the values of K_{Ic} derived from the J_{Ic} numbers according to

$$K_{Ic} = \sqrt{EJ_{Ic}},$$

which is identical to Eq. (5) except that the term $1 - \nu^2$ has been omitted. (This omission will be discussed subsequently.) The mean value of the K_{Ic} numbers, based on 1-percent extension, for all geometries tested is 32.8 ksi$\cdot\sqrt{\text{in.}}$, and the maximum deviation from this mean is only about 4 percent. The mean K_{Ic} value at the onset of crack growth

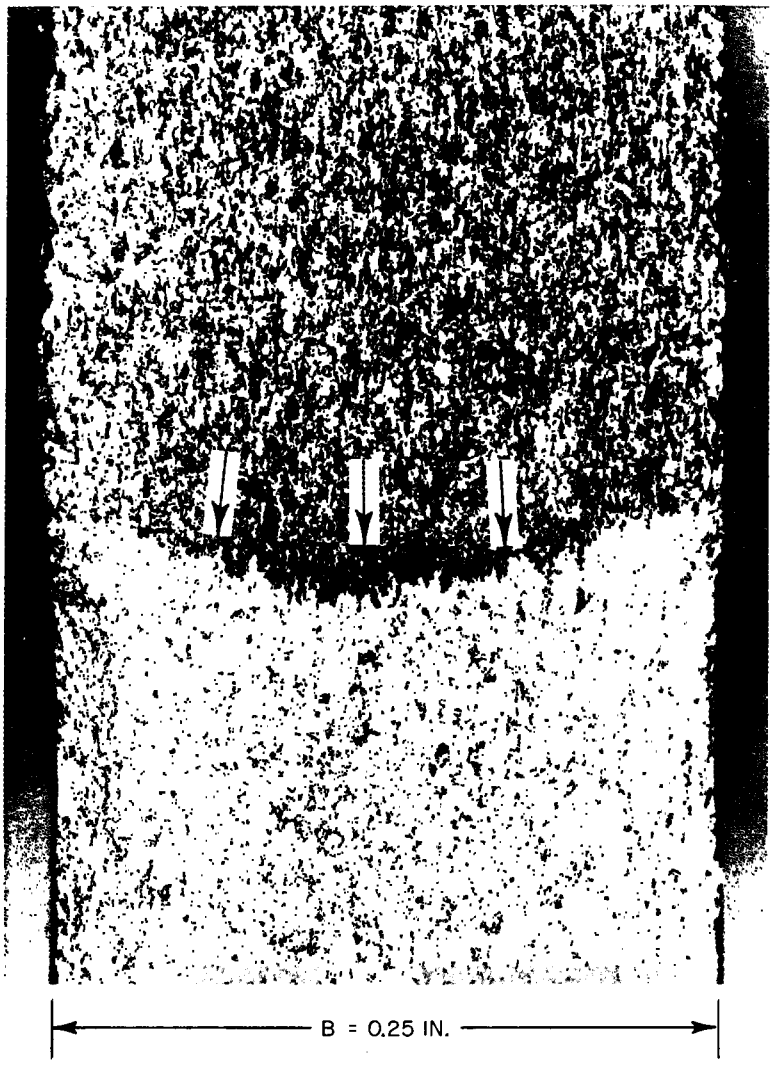

Fig. 10 — Crack extension in a 0.25-in.-thick 2024-T351 aluminum specimen. Arrows denote the leading edge of the fatigue precrack.

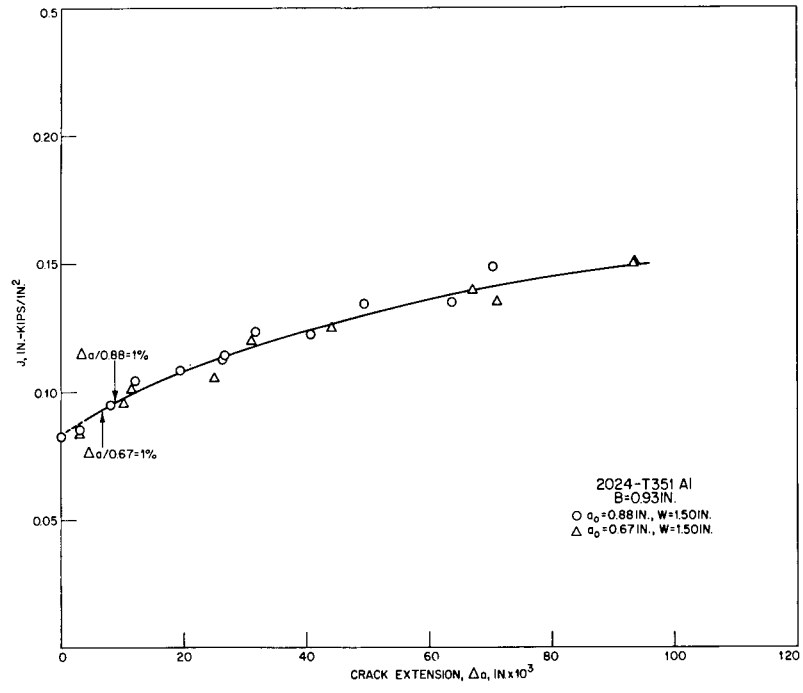

(a) 0.93-in.-thick specimens

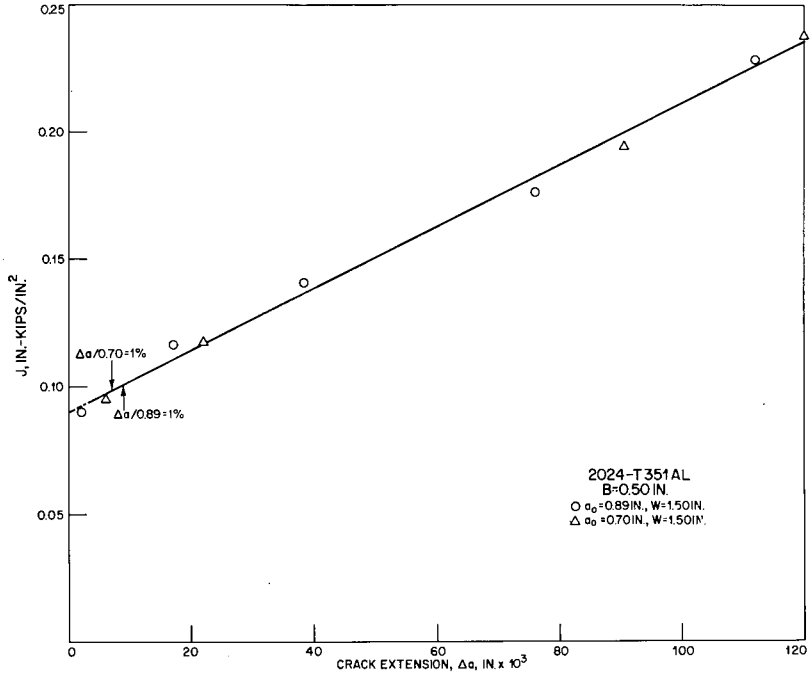

(b) 0.50-in.-thick specimens

Fig. 11 — J versus Δa for 2024-T351 aluminum specimens having a_0/W values of approximately 0.47 and 0.60

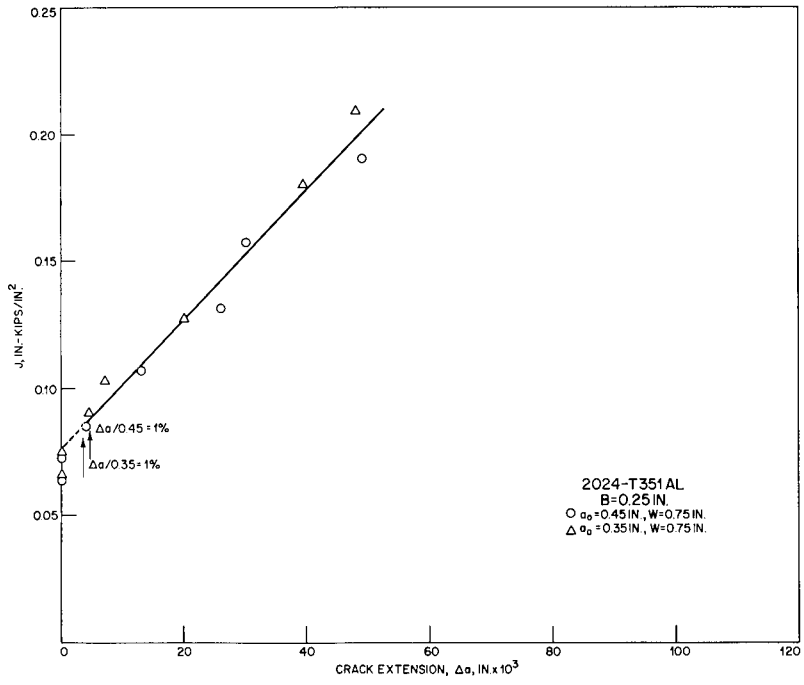

(c) 0.25-in.-thick specimens

Fig. 11 (Continued) — J versus Δa for 2024-T351 aluminum specimens having a_0/W values of approximately 0.47 and 0.60

Table 3
J_{Ic} Values for 2024-T351 Aluminum

B (in.)	a_0 (in.)	W (in.)	J_{Ic}* $\left(\frac{\text{in.}\cdot\text{kips}}{\text{in.}^2}\right)$	K_{Ic}† (ksi$\cdot\sqrt{\text{in.}}$)	J_{Ic}‡ $\left(\frac{\text{in.}\cdot\text{kips}}{\text{in.}^2}\right)$	K_{Ic}† (ksi$\cdot\sqrt{\text{in.}}$)	K_Q (ksi$\cdot\sqrt{\text{in.}}$)
0.25	0.45	0.75	0.0880	31.7	0.0770	29.7	20.9
0.25	0.35	0.75	0.0860	31.4	0.0770	29.7	20.0
0.50	0.89	1.50	0.101	34.0	0.0900	32.1	28.9
0.50	0.70	1.50	0.0985	33.5	0.0900	32.1	28.5
0.93	0.88	1.50	0.0965	33.2	0.0835	30.9	28.4
0.93	0.67	1.50	0.0935	32.7	0.0835	30.9	29.8

*1% crack extension.
†$K_{Ic} = \sqrt{J_{Ic}E}$.
‡Incipient crack growth.

(Δa = 0) is slightly lower: 30.9 ksi$\cdot\sqrt{\text{in.}}$, with a maximum deviation of less than 4 percent. For either definition of crack initiation the corresponding J_{Ic} (or K_{Ic}) values are remarkably invariant with specimen size, certainly well within the normal scatter of K_{Ic} numbers determined under linear elastic conditions. The K_Q values for this alloy (also shown in Table 3) vary from 20 to 30 ksi$\cdot\sqrt{\text{in.}}$ and, as mentioned previously, are of little significance.

Although the J_{Ic} values at 1-percent extension show little dependence on specimen dimensions in the present study, a significant size effect could become apparent in view of the observed invariance of the J-versus-Δa curve with initial crack length a_0. If the J-versus-Δa relationship were independent of a_0 over a sufficiently wide range of a_0 and if the J-versus-Δa curve were quite steep, then a fixed percentage of crack extension would lead to appreciably different J_{Ic} values for widely differing a_0. In view of the relatively small differences in a_0 used in the present study, this effect was not appreciable. However to circumvent potential difficulty for other materials and testing conditions, a definition of fracture initiation based on incipient growth may in general be the most useful.

In their studies on steels Begley and Landes [2,3] found that the J integral, like LEFM, has its limitations. When the specimen thickness or uncracked ligament ($W - a$) became sufficiently small, a dependence of the critical J-integral value on specimen size was encountered. Therefore these investigators suggested that J_{Ic} determination should be restricted to specimens having B and $W - a > 25J_{Ic}/\sigma_y$. Application of this criterion to the present study indicates that B and $W - a$ should exceed 0.049 in., which (Table 3) is met for all specimen configurations. Thus the geometry-independent J-integral values obtained are consistent with the proposed specimen size limitations.

In converting the J_{Ic} numbers (Table 3) to equivalent K_{Ic} values a state of plane stress rather than plane strain was assumed; that is, the quantity $1 - \nu^2$ was omitted from Eq. (5). Justification for this assumption is presented in Fig. 12, which shows the dependence of elastic stiffness $P/\delta EB$ on relative notch depth a_0/W. The experimental results were obtained from both bluntly notched and fatigue-cracked bend bars having the indicated dimensions. Also shown are the theoretical [9] linear elastic results for both plane-stress and plane-strain deformations. Although it is generally expected [12] that experimental results will fall between the plane-stress and plane-strain idealizations, the present data lie close to but slightly below the plane-stress solution. Hence, for consistency with linear elastic behavior, a state of plane stress was assumed in the present investigation.

Figure 13 is a composite of the J-versus-Δa curves shown separately in Fig. 11. The solid points represent the J values associated with the maximum load P_{max} on the load-versus-deflection diagram, and the open symbols represent the J-integral numbers at 1-percent crack growth. It is evident that the J values at P_{max} exceed those at initiation by 35 to 100 percent, depending on specimen size and the particular definition of fracture initiation adopted (incipient growth or 1-percent extension). Hence for this alloy the J-integral numbers at P_{max} neither approximate those at initiation nor do they stand alone as a separate, geometry-independent property of the metal. For rotor and pressure vessel steels however Begley and Landes [2,3] observed that no appreciable crack extension preceded P_{max} in tests conducted both in tension and bending. In such instances determination of P_{max} is a valid and straightforward method of obtaining J_{Ic}.

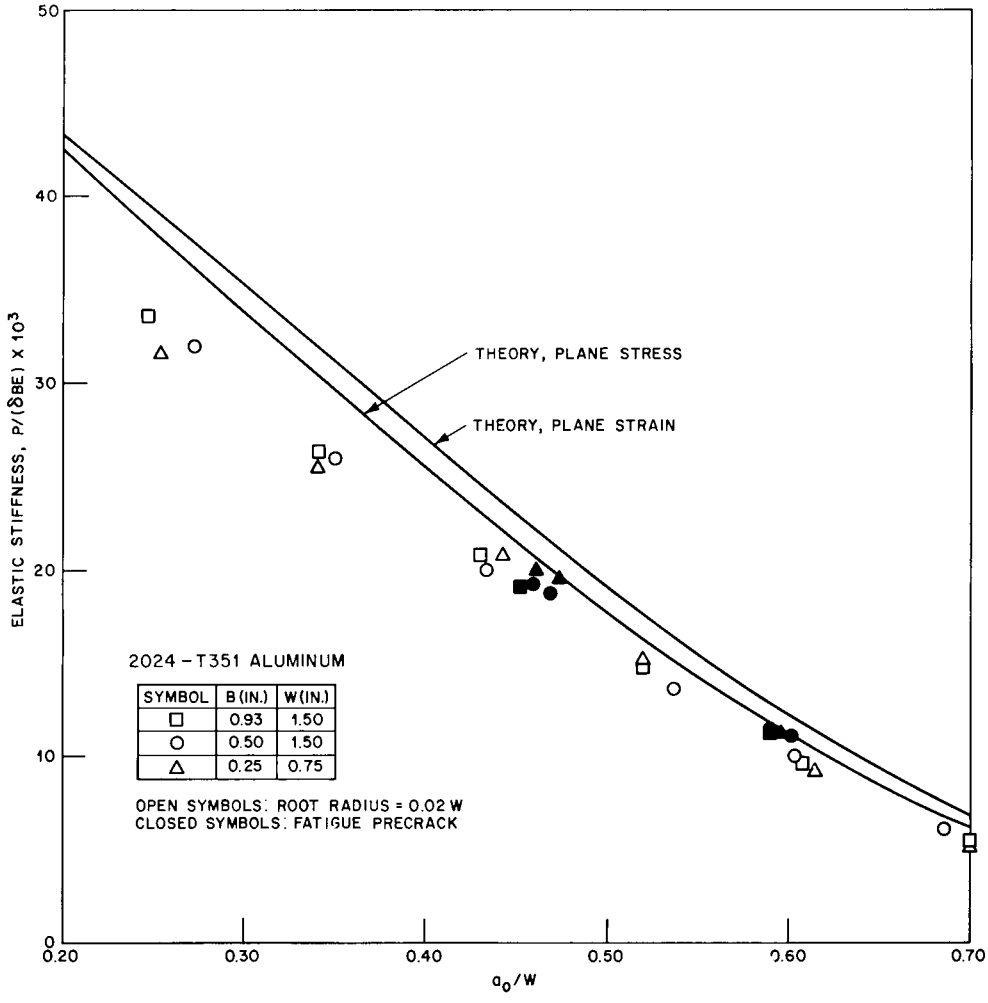

Fig. 12 — Dependence of elastic stiffness on relative crack depth for three-point bend specimens

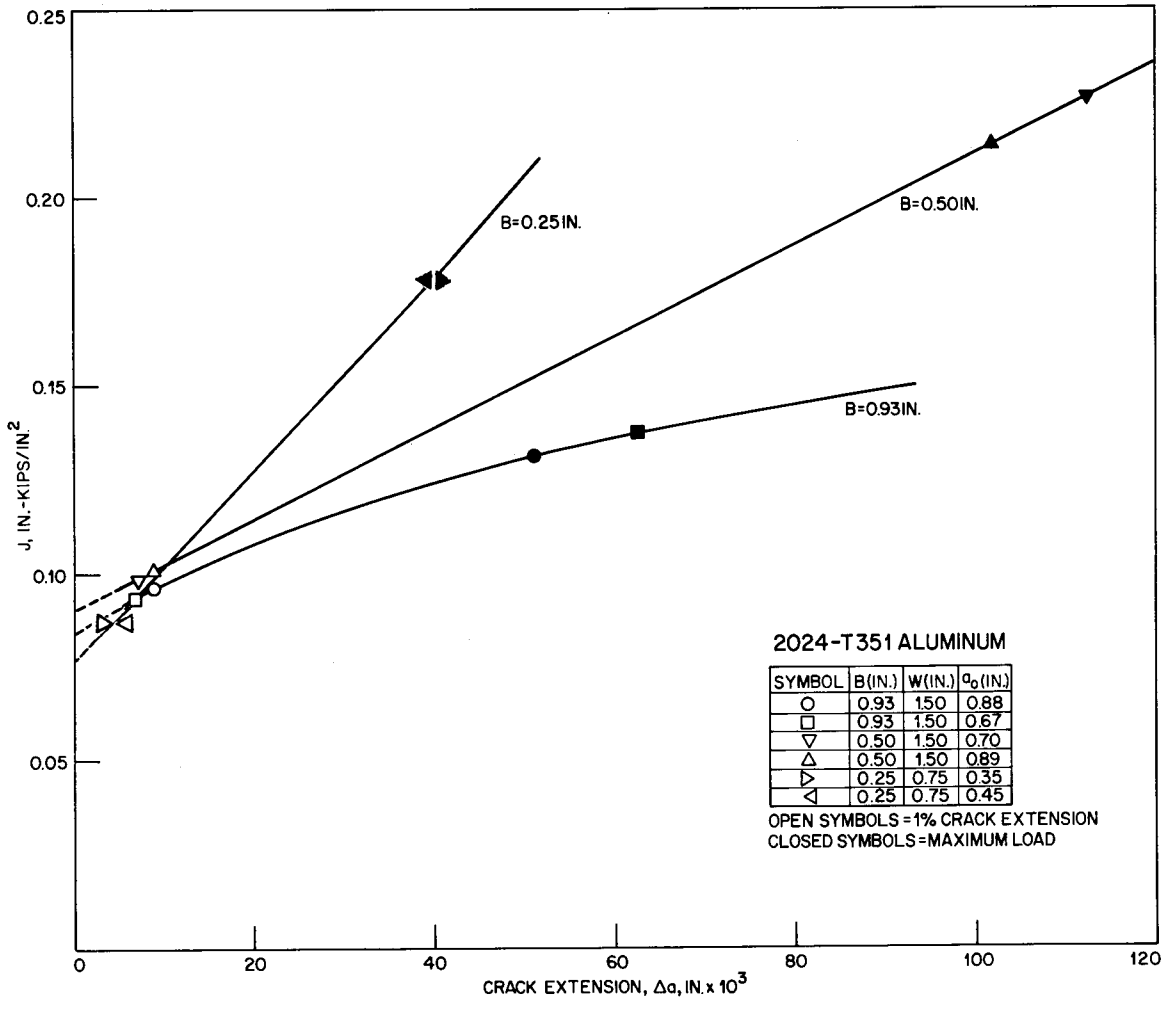

Fig. 13 — Composite of J-versus-Δa curves for 2024-T351 aluminum having thicknesses of 0.93, 0.50, and 0.25 in.

As indicated previously, the J-versus-Δa curves (summarized in Fig. 13) were found to be independent of initial crack size for a given thickness. Furthermore the average slopes of these curves are larger for the thinner specimens. These observations are consistent with the resistance-curve (R-curve) concept of fracture developed by Krafft et al. [13] for high-strength sheet materials. The R-curve approach relies on the experimental observations [14] that the relationship between the strain energy release rate G, measured under nominally elastic conditions, and Δa is a characteristic of the metal for a given thickness, that is, independent of planar dimensions and mode of loading. However, whether the J-versus-Δa relationship is exactly equivalent to the R-curve of LEFM remains to be determined. From a theoretical standpoint some question regarding this correspondence exists, because the J-integral approach is based on a linear-elastic approximation to metal plasticity, which is not valid once crack growth (local unloading) commences. The inverse relationship between the slope of the J-versus-Δa plot and specimen thickness is also in qualitative agreement with the observations of Pellini and Judy [15] and Goode and Judy [16], who have used energy data from dynamic-tear tests to characterize the influence of specimen size on fracture extension resistance.

SUMMARY

The primary conclusions to be drawn from this investigation are as follows:

- The J integral provides a quantitative, geometry-independent characterization of the fracture initiation resistance of 2024-T351 aluminum alloy. The mean value of K_{Ic} derived from six J_{Ic} values, measured at the onset of crack extension, is 30.9 ± 1.2 ksi·$\sqrt{\text{in.}}$. For the specimen geometries considered in the present study, determination of J_{Ic} at 1-percent crack extension also provides essentially constant K_{Ic} values (32.8 ± 1.4 ksi·$\sqrt{\text{in.}}$); however such an evaluation of J_{Ic} at a fixed percentage of the initial crack length may in some instances lead to a size effect in view of the observed independence of the J-versus-Δa relationship on initial crack length. As expected, linear elastic fracture mechanics (K_Q analysis) does not render meaningful stress intensity values, at least for section sizes below 1 in. thick.

- Heat tinting provides a straightforward means of documenting the amount of crack extension at selected points on the load-versus-deflection record. For materials which exhibit substantial crack growth prior to maximum load, such a means of crack extension measurement is necessary to define meaningful J_{Ic} values at initiation. Use of the maximum load point in determining J_{Ic} is not acceptable for these materials.

- The analytical procedure developed by Bucci et al. for determination of the J-integral calibration yields results which are within 10 percent of those determined experimentally. For most applications this discrepancy is acceptable and the analytical procedure can be of considerable value by eliminating the costly and time-consuming process of measuring a large number of load-versus-deflection curves.

- The J-versus-Δa curves for this alloy were found to depend only on specimen thickness over the range of initial crack sizes investigated. This feature of the J-versus-Δa relationship is consistent with the classical R-curve concept currently employed for

high-strength sheet alloys tested under nominally elastic conditions. However a rigorous equivalence of the two relationships remains to be established. The increase in slope of the J-versus-Δa curve with decreasing specimen thickness is consistent with prior observations made at NRL in which dynamic-tear energy is adopted as a measure of fracture extension resistance.

ACKNOWLEDGMENTS

The authors gratefully acknowledge the technical assistance of Mr. S. J. McKaye and the financial support provided by the Office of Naval Research. The authors are further indebted to Drs. G. R. Irwin and F. J. Loss for their advice during the formative stages of this work.

REFERENCES

1. J.R. Rice, "A Path Independent Integral and the Approximate Analysis of Strain Concentration by Notches and Cracks," Trans. ASME, J. Applied Mechanics 35 (1968), 379-386.
2. J.A. Begley and J.D. Landes, "The J Integral as a Fracture Criterion," ASTM STP 514, Am. Soc. Testing Mat., Philadelphia, 1972, pp. 1-20.
3. J.D. Landes and J.A. Begley, "The Effect of Specimen Geometry on J_{Ic}," ASTM STP 514, Am. Soc. Testing Mat., Philadelphia, 1972, pp. 24-39.
4. J.W. Hutchinson, "Singular Behavior at the End of a Tensile Crack in a Hardening Material," Journal of the Mechanics and Physics of Solids **16** (1968) pp. 13-31.
5. J.R. Rice and G.F. Rosengren, "Plane Strain Deformation Near a Crack Tip in a Power-Law Hardening Material," Journal of the Mechanics and Physics of Solids **16** (1968), pp. 1-12.
6. F.A. McClintock, "Plasticity Aspects of Fracture," Chapter 2 in *Fracture*, H. Liebowitz, editor, Vol. III, Academic Press, New York, 1968, pp. 47-225.
7. J.R. Rice, "Mathematical Analysis in the Mechanics of Fracture," Chapter 3 in *Fracture*, H. Liebowitz, editor, Vol. II, Academic Press, New York, 1968, pp. 191-311.
8. E399-72, "Standard Method of Test for Plane-Strain Fracture Toughness of Metallic Materials," *1972 Annual Book of ASTM Standards*, Part 31, Am. Soc. Testing Mat., Philadelphia, 1972, pp. 955-974.
9. R.J. Bucci, P.C. Paris, J.D. Landes, and J.R. Rice, "J Integral Estimation Procedures," ASTM STP 514, Am. Soc. Testing Mat., Philadelphia, 1972, pp. 40-69.
10. W.F. Brown, Jr., and J.E. Srawley, "Plane Strain Toughness Testing of High Strength Metallic Materials," ASTM STP 410, Am. Soc. Testing Mat., Philadelphia, 1966.
11. S. Timoshenko, *Strength of Materials*, Part I, Van Nostrand, Princeton, N.J., 1955, pp. 312-319.

12. B. Gross, E. Roberts, Jr., and J.E. Srawley, "Elastic Displacements for Various Edge-Cracked Plate Specimens," International Journal of Fracture Mechanics 4 (1968), pp. 267-276.

13. J.M. Krafft, A.S. Sullivan, and R.M. Boyle, "Effect of Dimensions on Fast Fracture Instability of Notch Sheets," Proc of the Crack Propagation Symposium, Vol. 1, Cranfield, England, 1961, pp. 8-29.

14. R.H. Heyer, "Crack Growth Resistance Curves (R-Curves) — Literature Review," presented at a meeting of ASTM Committee E-24, Hawthorne, California, 1971.

15. W.S. Pellini and R.W. Judy, Jr., "Significance of Fracture Extension Resistance (R-Curve) Factors in Fracture-Safe Design for Nonfrangible Metals," NRL Report 7187, Oct. 1970.

16. R.J. Goode and R.W. Judy, Jr., "Fracture Extension Resistance (R-Curves) Features of Nonfrangible Aluminum Alloys," NRL Report 7262, June 1971.